Local Dynamic Shimming for Slice-wise Image Acquisition

J-J. Hsu[1], G. H. Glover[1]
[1]Lucas Center for Imaging, Stanford University School of Medicine, Stanford, California, United States

Introduction. The shims of conventional clinical scanners usually are not able to correct the field inhomogeneity to a satisfactory level for region of interest (ROI) where the inhomogeneity is caused by local structure of smaller scale than the desired field of view. It is shown [1–5] that the shimming deficiency can be compensated by local shim field generated either passively by diamagnetic substance or actively by electric currents. The external magnetic field B_0 in the human inferior portion of the frontal lobe (IFL) is seriously distorted and needs to be corrected for fMRI. Previously, we have shown [4,5] that local shimming for IFL can be effectively achieved by current carrying coils held in the subject's mouth. In developing local shimming [4–6], it was noted that better shimming results by dividing the ROI into smaller regions and shim and acquire each region's image separately. In this work, we report an implementation of local dynamic shimming and explore its advantage over static shimming. The results show that dynamic shimming will be very helpful in fMRI or imaging in which the data are acquired slice-wise.

Methods. The details of the local shimming are given in Ref. [5]. In short, a set of coils are held in the subject's mouth; then, a series of MRI B_0 maps are constructed to determine the magnet field each coil can generate. The scanner operator prescribes an ROI and the pixels in the ROI are used to compute the shim currents through a linear least-square fitting and based on the B_0 maps. Thus the shimming field is optimized for the ROI of the operator's choice. In slice-wise dynamic shimming, the ROI is divided into slices and the shim currents as well as the B_0 shift (Z_0 shim) are computed for each slice. In the present implementation, the B_0 shifts are loaded in the pulse sequencer's memory and added to the RF frequency in accordance with the slice being scanned. The values of the shim currents are stored in a table of a control program (E-Prime, PST) running on a personal computer. During a multi-slice MRI, the scanner triggers the personal computer by a TTL signal ~10 ms (depending on the repetition time T_R) each time before a slice is selected. The control program then updates the output of a multi-channel shim power supply (MXA, Resonance Research) by commands transmitted through an RS232 serial connection. The experiment was carried out at 1.5 T with a clinical scanner (Excite, GE Healthcare). No artifact caused by the changing of shim currents has been observed.

Results and Discussion. Referred to Fig 1, an ROI in each of slices 2, 3, and 4 was prescribed targeting at the IFL. In volume shimming, the shim currents were optimized for all the ROIs as a whole. In slice-wise dynamic shimming, the currents were optimized for each ROI and output when the corresponding slice was being acquired. As shown in Fig 1, both volume and dynamic shimming have recovered lost signal considerably (for example, in slice 3). Slice 1 was not prescribed for shimming. However, because the shim current stayed constant during the entire scan in volume shimming, the image of slice 1 was distorted by the shim field (see the area pointed by the arrow in Fig 1c), while in dynamic shimming, the image remained the same as that without local shimming. The effectiveness and flexibility of local dynamic shimming can further be appreciated in the example in Fig 2. Figure 2a is a mid-sagittal B_0 map constructed from two gradient-echo MRI scans of different echo time T_E; the box indicates the ROI for the shim current computation. By using the Biot–Savart's law, the resultant shim field is computed (neglecting boundary conditions) for various shim-coil locations and added to the B_0 map of Fig 2a. Figure 2b is the shimmed B_0 map for a single, circular oral shim coil of 1.6-cm diameter; the B_0 root-mean-square (RMS) in the ROI is reduced to 65%. In Fig 2c, the shim coil consists of two circular coils of 4-cm diameter with axes at 60° and 120° azimuth; the RMS reduction is 64%, comparable to the oral shim coil, but the field outside the ROI is distorted. Nevertheless such shim coil at non-ideal but easily accessible location [5] can still be considered in coil design in dynamic shimming, making the design convenient and flexible. Although the current study is focused on the brain for fMRI; other areas of problematic geometry may benefit from local dynamic shimming as well, for example, the neck, shoulders, and breasts.

Acknowledgements. This work is supported by NIH RR09784 and the Richard M. Lucas Foundation.

References: [1] JL Wilson *et al*., Magn Reson Med **48**, 906 (2002); Neuroimage **19**, 1802 (2003). [2] V Roopchansingh *et al.*, In: Proc 12th ISMRM, 1650 (2004). [3] EC Wong and Y Mazaheri, In: Proc 12th ISMRM, 520 (2004). [4] J-J Hsu and GH Glover, In: Proc 11th ISMRM, 734 (2003); In: Proc 12th ISMRM, 994 (2004). [5] J-J Hsu and GH Glover, Magn Reson Med **53** 243 (2005). [6] J-J Hsu and GH Glover, In: Proc 13th ISMRM, 1535 (2005).

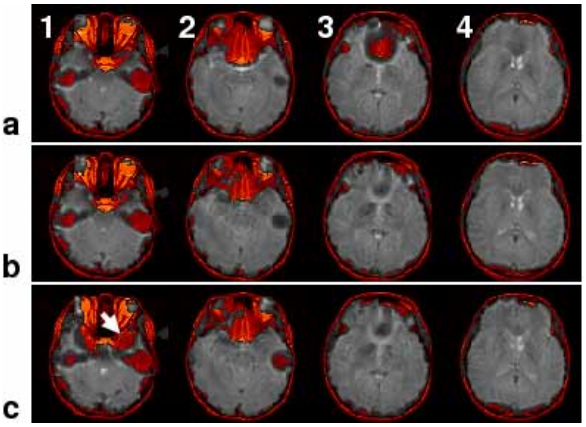

◄ **Figure 1** Comparison of effect of local shimming. (**a**) no local shimming, (**b**) with local, dynamic slice-wise shimming, (**c**) with local, static volume shimming. The spiral images (gray; T_E = 40 ms) are overlaid with fast-spin-echo anatomic images (red) for easy identification of signal recovery.

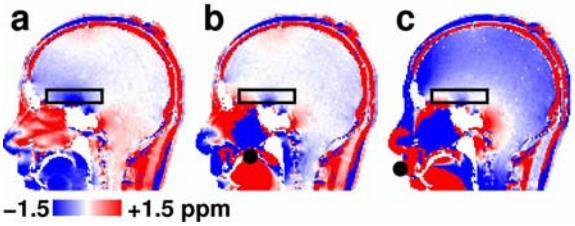

▲ **Figure 2** B_0 maps for comparison of shimming effectiveness. The shim coil locations are marked by black dots.